J. Fluid Mech. (1996), *vol.* 317, *pp.* 129–154

Simple cases of the streamline-curvature instability in three-dimensional boundary layers

By NOBUTAKE ITOH
National Aerospace Laboratory, Chofu, Tokyo, Japan

(Received 4 July 1995 and in revised form 6 November 1995)

A new instability of the centrifugal type due to the curvature of external streamlines was theoretically predicted in a recent study on boundary layers along a swept wing. It is, however, not clear how this instability relates to already-known instability phenomena in various three-dimensional flows. So the basic idea developed in the analysis of boundary layers is applied to the simpler problems of the flow on a rotating disk and along the leading edge of a yawed circular cylinder, and the resulting eigenvalue problems are numerically solved to show multiple stability characteristics of the flows. Computational results confirm that the streamline-curvature instability does appear in the rotating-disk flow and that it is in fact identical with the instability called the 'parallel' or 'type 2' mode in the atmospheric literature. This instability is also found to occur in the steady flow near the attachment line and to give the lowest values of the critical Reynolds number except for a very narrow region close to the attachment line, where the viscous and cross-flow instabilities are dominant. These facts provide evidence to show that the same mode of instability as the classical one observed in rotating flows can appear in general three-dimensional boundary layers without rotation.

1. Introduction

The study of the process of instability and transition to turbulence in boundary layers developing on a swept wing is very important in fluid dynamics and aeronautical science, because knowledge of those phenomena is indispensable for practical application of the methods of transition prediction and the technology of boundary-layer control to high-speed aircrafts. Those boundary layers are three-dimensional in the sense that streamlines of external inviscid flow are curved in the plane parallel to the wall by the different directions of the main stream and pressure gradient, and thereby the velocity in the viscous layer has a cross-flow component normal to the external flow. Because of this, three-dimensional boundary layers show very complicated characteristics even in the initial stage of transition. That is, some different kinds of instabilities can appear there and invite much earlier transition to turbulence than in two-dimensional boundary layers. It is of particular importance that some of those instabilities are inherent in three-dimensional flows and occur in the region near the leading edge of a wing, because this may be responsible for the early transition of three-dimensional boundary layers. Since our knowledge of the multiple instabilities is still insufficient, further studies to clarify detailed properties of each phenomenon are necessary for meeting increasing engineering needs.

In experiments on three-dimensional boundary layers along swept wings, two kinds of instabilities have been observed, one being the Tollmien–Schlichting instability

commonly seen in two-dimensional flows and the other the cross-flow instability induced by the existence of an inflexion point in the twisted velocity distribution. Classical instability theory based on the Orr–Sommerfeld equation (Mack 1984; Itoh 1991) indicates that the cross-flow instability occurs in the front region of negative pressure gradient near the leading edge and the Tollmien–Schlichting instability governs the rear region of zero or positive pressure gradient. However, a recent study by the present author (Itoh 1994*b*) has predicted theoretically that a new instability due to the curvature of external streamlines can occur in three-dimensional boundary layers on a swept wing. This instability is likely to appear in the region closer to the leading edge than the cross-flow instability. In fact, subsequent studies (Itoh 1995, 1996) used a combination of an approximate boundary-layer calculation based on the momentum integral equation and a simple method of linear stability calculation including the principal effects of wall and streamline curvatures, and determined critical Reynolds numbers of the multiple instabilities in the simplest flows on a yawed circular and elliptic cylinders. The results show that the flow region along a cylinder is divided into three subregions as one moves from the leading edge, governed by respectively the streamline-curvature instability, the cross-flow instability and the Tollmien–Schlichting instability.

Another important example of three-dimensional boundary layers is the flow on a rotating disk, because it includes the curvature of the flow field and the cross-flow component of velocity. Gregory, Stuart & Walker (1955) made both experimental observations and a theoretical analysis of the rotating-disk flow and revealed some fundamental properties of its instability. Their comparison between theory and experiment showed that stationary vortices are produced by an inviscid instability of the inflexion-point type caused by the existence of cross-flow. About ten years later, another kind of instability was found by Faller & Kaylor (1966) and Lilly (1966) in experiments and stability calculations, respectively, of the rotating-disk flow and the Ekman boundary layer. This instability occurs even at a much lower Reynold number than the critical value of the cross-flow instability and induces travelling waves with wavenumbers quite different from the wavenumber region of the cross-flow vortices. Recent studies by Balakumar & Malik (1990), Balakumar, Malik & Hall (1991) and Faller (1991) gave detailed results of linear stability computations which shed light on various aspects of the multiple instabilities in the rotating-disk flow.

For the situation described above, we have two straight-forward questions on the new instability induced by the curvature of external streamlines. One is whether or not this instability can occur in rotating flows, where the curvature of the flow field becomes infinitely large as the distance from the rotation axis decreases to zero. At present, there are no experimental observations of the streamline-curvature instability in boundary layers on swept wings, so evidence should be sought for this new instability in the rotating-disk flow. This investigation will contribute to the clarification of the relation between the instabilities already observed in the rotating flow and the new one predicted for general boundary-layer flows without rotation. The second question is how the streamline-curvature instability behaves in the flow near the attachment line on a swept wing. It should be noted that the previous calculations of the new instability excluded the region very close to the leading edge of a wing, because of doubt about whether the approximate disturbance equations used were applicable to this region. The stability problem of the attachment-line flow near the leading edge is, of course, itself very important and has received much attention from investigators, because the transition process in downstream boundary-layer flows would be affected markedly by instability of this leading flow (see Poll, 1984, 1985 and Reed & Saric 1989

for simple reviews). However, in the present circumstances we expect understanding of the associated phenomena to be advanced by the new concept of streamline-curvature instability. It is of particular practical interest to examine relations between the instability phenomena of the attachment-line flow and those of the fully developed boundary-layer flow downstream, say, on a yawed circular cylinder.

The present study, stimulated by the above questions, is a linear analysis to show the most important mechanisms and fundamental properties of the multiple instabilities in the flows on a rotating disk and along an attachment line, with particular attention to the principal effects of the curvature of external streamlines. Two kinds of formulation are presented to describe those effects: one is the simplest form directly applicable to rotating flows and the other is a modified one for convenience of application to the flow on a slender swept wing. Then eigenvalue problems posed by the resulting ordinary differential systems are solved numerically to determine local critical Reynolds numbers and principal stability characteristics as functions of a parameter characterizing the basic flow. The numerical results will be compared with those obtained for the rotating-disk and boundary-layer flows in the existing studies quoted above, in the expectation that we have useful information on the streamline-curvature instability. Although rather rough approximations are used in the analysis, the simplicity of the formulation is very convenient for clarification of the essential mechanism of the phenomena and for seeing the most fundamental properties of the instabilities.

The next two sections present the simplest form of the disturbance equations for describing the streamline-curvature instability and the results of application to the rotating-disk flow as well as comparison with existing theories. In §§4 and 5, a similar but more convenient form of the disturbance equations is derived for the stability analysis of the flow on a yawed circular cylinder. On the basis of the numerical results, we discuss the main effects of the streamline curvature on critical Reynolds numbers and stability characteristics of the attachment-line flow in §6. Some concluding remarks are presented in the final section.

2. Model equations describing the streamline-curvature instability

We start by deriving the simplest form of the disturbance equations that can describe the streamline-curvature instability, because it will be helpful in understanding the essential mechanism of the new instability. For this purpose, it is convenient to consider a three-dimensional laminar boundary layer on a stationary horizontal plane under a potential flow whose streamlines have a local radius of curvature r_0 and to assume that the growth of the boundary-layer thickness can be ignored at least at the level of approximation concerned. These conditions are satisfied in the problem of rotating-disk flow, which will be discussed in the next section. It is also convenient for an explicit representation of the curvature to use the cylindrical polar coordinate system with the vertical axis located at the centre of the curvature. Let (r, θ, z) denote the coordinates, t time, (v_r, v_θ, v_z) velocity components, p^* pressure, ρ density and ν kinematic viscosity. Attention is here directed to a close vicinity of a reference point $(r_0, \theta_0, 0)$ on the plane, and the boundary-layer thickness is denoted by a constant δ, the reference length in the horizontal directions by L, the reference velocity by Q_0, and the Reynolds number is defined by $R = Q_0 \delta/\nu$. In addition, we introduce two non-dimensional parameters defined by $\epsilon_0 = \delta/L$ and $\kappa = \delta/r_0$, where ϵ_0 is a small parameter inversely proportional to the Reynolds number and κ denotes dimensionless curvature of the external streamline and is also assumed to be very small. Then all other quantities are made dimensionless as

$$\left.\begin{aligned} &r_0(\theta-\theta_0)/L=-\xi, \quad (r-r_0)/L=\eta, \quad z/\delta=\zeta, \quad Q_0 t/L=\tau,\\ &v_\theta/Q_0=-U(\zeta;\xi,\eta)-\mathrm{Re}\,[u(\zeta;\xi,\eta)\exp(\mathrm{i}\Theta/\epsilon_0)],\\ &v_r/Q_0=V(\zeta;\xi,\eta)+\mathrm{Re}\,[v(\zeta;\xi,\eta)\exp(\mathrm{i}\Theta/\epsilon_0)],\\ &v_z/Q_0=\epsilon_0 W(\zeta;\xi,\eta)+\mathrm{Re}\,[w(\zeta;\xi,\eta)\exp(\mathrm{i}\Theta/\epsilon_0)],\\ &p^*/(\rho Q_0^2)=P(\xi,\eta)+\mathrm{Re}\,[p(\xi;\zeta,\eta)\exp(\mathrm{i}\Theta/\epsilon_0)], \end{aligned}\right\} \tag{2.1}$$

where negative signs in front of ξ, U and u have been introduced to yield the right-hand system of coordinates, (u,v,w,p) denote the small disturbance superimposed on the basic flow (U,V,W,P) and Re denotes the real part, while ξ and η may be assumed to be of order ϵ_0, because we consider a close vicinity of the reference point. Partial derivatives of the phase function $\Theta(\xi,\eta,\tau)$ define the real wavenumbers in the ξ- and η-directions and the complex frequency as

$$\alpha=\frac{\partial\Theta}{\partial\xi}, \quad \beta=\frac{\partial\Theta}{\partial\eta}, \quad \omega=-\frac{\partial\Theta}{\partial\tau}, \tag{2.2}$$

respectively, where non-dimensionalization has been made with the boundary-layer thickness δ because of scaling the exponent with ϵ_0. Substituting the above into the continuity and Navier–Stokes equations written in cylindrical coordinates, subtracting the basic-flow parts, which are assumed to satisfy the equations of motion by themselves, and neglecting coupling terms of the small disturbance, we have linear disturbance equations of the form

$$\frac{1}{h}\left(\mathrm{i}\alpha+\epsilon_0\frac{\partial}{\partial\xi}\right)u+\left(\mathrm{i}\beta+\epsilon_0\frac{\partial}{\partial\eta}+\frac{\kappa}{h}\right)v+\mathrm{D}w=0, \tag{2.3a}$$

$$\left[\frac{1}{R}\left(\nabla^2-\frac{\kappa^2}{h^2}\right)+\mathrm{i}\omega-\frac{U}{h}\left(\mathrm{i}\alpha+\epsilon_0\frac{\partial}{\partial\xi}\right)-V\left(\mathrm{i}\beta+\epsilon_0\frac{\partial}{\partial\eta}\right)-\epsilon_0 W\mathrm{D}-\frac{\epsilon_0}{h}\frac{\partial U}{\partial\xi}-\frac{\kappa}{h}V\right]u$$
$$+\left[\frac{2\kappa}{Rh^2}\left(\mathrm{i}\alpha+\epsilon_0\frac{\partial}{\partial\xi}\right)-\epsilon_0\frac{\partial U}{\partial\eta}-\frac{\kappa U}{h}\right]v-\mathrm{D}Uw-\frac{1}{h}\left(\mathrm{i}\alpha+\epsilon_0\frac{\partial}{\partial\xi}\right)p=0, \tag{2.3b}$$

$$\left[\frac{1}{R}\left(\nabla^2-\frac{\kappa^2}{h^2}\right)+\mathrm{i}\omega-\frac{U}{h}\left(\mathrm{i}\alpha+\epsilon_0\frac{\partial}{\partial\xi}\right)-V\left(\mathrm{i}\beta+\epsilon_0\frac{\partial}{\partial\eta}\right)-\epsilon_0 W\mathrm{D}-\epsilon_0\frac{\partial V}{\partial\eta}\right]v$$
$$+\left[-\frac{2\kappa}{Rh^2}\left(\mathrm{i}\alpha+\epsilon_0\frac{\partial}{\partial\xi}\right)-\frac{\epsilon_0}{h}\frac{\partial V}{\partial\xi}+\frac{2\kappa U}{h}\right]u-\mathrm{D}Vw-\left(\mathrm{i}\beta+\epsilon_0\frac{\partial}{\partial\eta}\right)p=0, \tag{2.3c}$$

$$\left[\frac{1}{R}\nabla^2+\mathrm{i}\omega-\frac{U}{h}\left(\mathrm{i}\alpha+\epsilon_0\frac{\partial}{\partial\xi}\right)-V\left(\mathrm{i}\beta+\epsilon_0\frac{\partial}{\partial\eta}\right)-\epsilon_0 W\mathrm{D}-\epsilon_0\mathrm{D}W\right]w$$
$$-\frac{\epsilon_0^2}{h}\frac{\partial W}{\partial\xi}u-\epsilon_0^2\frac{\partial W}{\partial\eta}v-\mathrm{D}p=0, \tag{2.3d}$$

where $h=1+\kappa(\eta/\epsilon_0)$ may be assumed to be $1+O(\kappa)$ and the differential operators are defined by $\mathrm{D}=\partial/\partial\zeta$ and

$$\nabla^2=\mathrm{D}^2+\frac{1}{h^2}\left(\mathrm{i}\alpha+\epsilon_0\frac{\partial}{\partial\xi}\right)^2+\left(\mathrm{i}\beta+\epsilon_0\frac{\partial}{\partial\eta}\right)^2+\frac{\kappa}{h}\left(\mathrm{i}\beta+\epsilon_0\frac{\partial}{\partial\eta}\right).$$

Since the main purpose of the present study is to clarify the most important effects of the streamline curvature on the instability of a three-dimensional flow, we wish to

reduce the above partial differential equations to an ordinary differential system, which poses an eigenvalue problem commonly applicable to the different types of instability mentioned earlier and enables us to make a simple estimation of the stability characteristics of a given flow. In practice, we follow the basic idea of the previous work (Itoh 1994*b*) and construct a model system by retaining only the most important terms in the original equations. If the magnitude of the principal inviscid terms $\omega-\alpha U-\beta V$ is denoted by a non-dimensional parameter ϵ, then ϵ is of order unity for the two-dimensional Tollmien–Schlichting waves but is zero for the neutrally stable state of Taylor–Görtler vortices in two-dimensional flows, because the former have the wavenumber vector parallel to the basic flow but the wavenumber vector of the latter is perpendicular to the basic flow. In three-dimensional boundary layers with small cross-flows, ϵ takes non-zero values in the range from order unity to order much smaller than unity according to the type of disturbances; in particular for the disturbance whose wavenumber vector is perpendicular to the external stream, this parameter is considered to represent the magnitude of the cross-flow V, which may be taken to be smaller than unity but larger than ϵ_0 for general boundary layers. On the other hand, it is obvious from the classical theory of linear stability that the viscous terms $R^{-1}(\mathrm{D}^2-\alpha^2-\beta^2)$ become so large as to balance with the principal inviscid terms of $O(\epsilon)$ in the critical and wall layers and play an important role at least in the viscous Tollmien–Schlichting instability of boundary-layer flows, although R^{-1} is itself of $O(\epsilon_0)$. Furthermore, an order analysis gives rise to the fact that the principal curvature term is given only by $2\kappa Uu$ in (2.3*c*) and becomes important in the equations for $\epsilon=\kappa^{1/2}$, showing a striking similarity to the corresponding wall-curvature term in the Taylor–Görtler instability. To incorporate the principal inviscid, viscous and curvature terms discussed in a plausible and plain formulation, we introduce the orders of magnitude as

$$\left.\begin{aligned} &1\geqslant\epsilon\geqslant\kappa^{1/2}>\epsilon_0, \quad U,u,\beta\sim O(1),\\ &V,v,w,\alpha,\omega,R^{-1}\sim O(\epsilon), \quad p\sim O(\epsilon^2), \end{aligned}\right\} \tag{2.4}$$

where R^{-1} represents only the coefficients of the viscous terms in (2.3), being distinguished from the other terms of $O(\epsilon_0)$. Then the magnitude of all terms in (2.3) is evaluated to derive the lowest-order approximations to the exact equations for different magnitudes of ϵ. This analysis shows that the largest curvature term $2\kappa Uu$ remains in the lowest-order approximation for $\epsilon=\kappa^{1/2}$ but that for larger values of ϵ all curvature terms become negligible and the leading-order equations for $1>\epsilon>\kappa^{1/2}$ are the same as those for $\epsilon=\kappa^{1/2}$ on dropping the curvature term. It is also found that we have the parallel-flow approximation equivalent to the Orr–Sommerfeld equation in another limit, $\epsilon=1$. Therefore, superposition of the results for the two limiting cases gives rise to model equations applicable to the whole range of $1\geqslant\epsilon\geqslant\kappa^{1/2}$. The resultant equations are:

$$\mathrm{i}\alpha u+\mathrm{i}\beta v+\mathrm{D}w=0, \tag{2.5a}$$

$$\left[\frac{1}{R}(\mathrm{D}^2-\alpha^2-\beta^2)+\mathrm{i}(\omega-\alpha U-\beta V)\right]u-U'w-\mathrm{i}\alpha p=0, \tag{2.5b}$$

$$\left[\frac{1}{R}(\mathrm{D}^2-\alpha^2-\beta^2)+\mathrm{i}(\omega-\alpha U-\beta V)\right]v-V'w+2\kappa Uu-\mathrm{i}\beta p=0, \tag{2.5c}$$

$$\left[\frac{1}{R}(\mathrm{D}^2-\alpha^2-\beta^2)+\mathrm{i}(\omega-\alpha U-\beta V)\right]w-\mathrm{D}p=0, \tag{2.5d}$$

where the prime denotes differentiation with respect to ζ. These equations are slightly different from and simpler than those previously obtained for boundary layers on a swept wing, because the growth of the boundary-layer thickness has been ignored here on the grounds of a constant thickness of the rotating-disk flow.

We have thus obtained a very simple ordinary-differential model of the original disturbance equations, but it is more convenient for numerical solution of the problem to eliminate v and p from the above equations on the assumption of β being not zero. This yields simultaneous equations for u and w of the form

$$\left[(\alpha^2+\beta^2)\left\{\frac{1}{R}(\mathrm{D}^2-\alpha^2-\beta^2)+\mathrm{i}(\omega-\alpha U-\beta V)\right\}-2\alpha\beta\kappa U\right]u$$
$$-\left[\mathrm{i}\alpha\left\{\frac{1}{R}(\mathrm{D}^2-\alpha^2-\beta^2)+\mathrm{i}(\omega-\alpha U-\beta V)\right\}\mathrm{D}+\beta(\beta U'-\alpha V')\right]w=0, \quad (2.6a)$$

$$\left[\left\{\frac{1}{R}(\mathrm{D}^2-\alpha^2-\beta^2)+\mathrm{i}(\omega-\alpha U-\beta V)\right\}(\mathrm{D}^2-\alpha^2-\beta^2)+\mathrm{i}(\alpha U''+\beta V'')\right]w$$
$$-2\mathrm{i}\beta\kappa(U\mathrm{D}+U')u=0. \quad (2.6b)$$

This form of the equations presents the simplest modification of the parallel-flow approximation and reduces to a three-dimensional version of the Orr–Sommerfeld equation if we put $\kappa=0$, and its simplicity is suitable for our purpose of extracting the pure effects of the streamline curvature from the complex effects of various factors appearing in the exact disturbance equations. The above equations are accompanied by the boundary conditions that disturbance velocities vanish on the wall and away from the wall, but it is again convenient for numerical solution to replace the outer conditions with the equivalent matching conditions imposed at an appropriate boundary-layer edge ζ_e. Outside the edge, U and V may be replaced with constant values U_0 and V_0, respectively, and the disturbance equations (2.6) reduce to the simpler ones including constant coefficients only. Then the usual procedure derives the conditions for the solution to decay far away from the wall, which may be written in the form of three differential relations to be satisfied by the outer solution everywhere in the outer field and at the same time by the inner solution at the boundary-layer edge. After some simplification based on the same level of approximation as before, we have the boundary conditions of the form

$$u=w=w'=0 \quad \text{at} \quad \zeta=0, \quad (2.7a)$$

$$u'+\rho_1 u+\frac{\mathrm{i}\alpha}{\rho_2(\rho_1-\rho_2)}(w''+2\rho_1 w'+\rho_1^2 w)=0, \quad (2.7b)$$

$$w''+(\rho_1+\rho_2)w'+\rho_1\rho_2 w+\frac{\mathrm{i}\beta R\kappa U_0}{\rho_1+\rho_2}u=0, \quad (2.7c)$$

$$w'''+(2\rho_1+\rho_2)w''+\rho_1(\rho_1+2\rho_2)w'+\rho_1^2\rho_2 w=0 \quad \text{at} \quad \zeta=\zeta_e, \quad (2.7d)$$

where $\rho_1=(\alpha^2+\beta^2-\mathrm{i}\omega R+\mathrm{i}\alpha R U_0+\mathrm{i}\beta R V_0)^{1/2}$ and $\rho_2=(\alpha^2+\beta^2)^{1/2}$.

The homogeneous set of the equations and boundary conditions given above constitutes an eigenvalue problem to determine the complex quantity ω as a function of the wavenumbers α and β, the Reynolds number R and the streamline curvature κ in the form

$$\omega=\omega(\alpha,\beta,R;\kappa). \quad (2.8)$$

Since the real and imaginary parts of ω denote frequency and temporal growth rate of

disturbances, respectively, the condition of neutral stability is given by $\mathrm{Im}[\omega] = 0$, which defines a surface in the three-dimensional space with the coordinates α, β and R. For a given value of κ, the critical point (α_c, β_c, R_c) is determined as the point where R takes a minimum on the surface and is obtained by solving the simultaneous equations

$$\mathrm{Im}[\omega(\alpha, \beta, R)] = \mathrm{Im}[\omega_\alpha(\alpha, \beta, R)] = \mathrm{Im}[\omega_\beta(\alpha, \beta, R)] = 0, \tag{2.9}$$

where the subscripts α and β denote partial differentiations. Computations of the eigenvalues and their partial derivatives with respect to α and β are made with a numerical method developed by the author (Itoh 1974; Watanuki & Itoh 1984). Preliminary calculations have been done with various locations of the boundary-layer edge to confirm that the dependence of eigensolutions on ζ_e becomes negligible if we take a sufficiently large distance $\zeta_e = 10$ (cf. Itoh 1994*a*), and this value has been adopted in the computation reported here.

3. Application to the flow on a rotating disk

In this section, the above model of disturbance equations is used to examine whether the streamline-curvature instability can occur in a rotating flow. If there is an instability that is described by the present system but not by the Orr–Sommerfeld equation, then we may consider that the instability is induced by the curvature of flow field, because our equation system forms the simplest modification of the Orr–Sommerfeld system with addition of a curvature term only. For the basic laminar flow on a sufficiently large disk rotating in the counter-clockwise direction with a constant angular velocity ω_D, we have an exact solution of the Navier–Stokes equations:

$$v_r = r\omega_D F'(\zeta), \quad v_\theta = r\omega_D\{G(\zeta)+1\}, \quad v_z = -2(\nu\omega_D)^{1/2}F(\zeta), \tag{3.1}$$

with the solution of the ordinary differential equations

$$\left.\begin{aligned} F'''+2FF''-(F')^2+(1+G)^2 = 0, \quad G''+2FG'-2F'(1+G) = 0, \\ F(0) = F'(0) = G(0) = 0, \quad F'(\infty) = 0, \quad G(\infty) = -1, \end{aligned}\right\} \tag{3.2}$$

where the vertical distance ζ has been made dimensionless with the boundary-layer thickness defined by $\delta = (\nu/\omega_D)^{1/2}$. For this basic flow, the reference length and the reference velocity associated with (2.1) are taken as $L = r_0$ and $Q_0 = r_0\omega_D$, respectively, so that the dimensionless curvature of streamlines is related to the Reynolds number by $\kappa = R^{-1}$. In our formulation, however, we regard these two parameters as being independent of each other. This defines a kind of false flow as a generalization of the real rotating-disk flow and provides information about the main effects of the streamline curvature separated from those of the Reynolds number. When the simplified disturbance equations (2.6) are applied to this basic flow, it is convenient for comparison with other theories to use the coordinate system rotating with the disk. The corresponding transformation results in the replacement of U and ω with $U-1$ and $\omega-\alpha$ in (2.6); in reality, only the term $2\kappa Uu$ is replaced with $2\kappa(U-1)u$ in the equations, where the basic flow is given by $U = -G(\zeta)$ and $V = F'(\zeta)$. We should note here that this replacement removes the curvature term from the boundary conditions (2.7), because the basic-flow part $U-1$ vanishes outside the boundary-layer edge, in striking contrast with the case of general three-dimensional boundary layers, where the outer boundary conditions include the curvature in the same way as in the Taylor–Görtler problem.

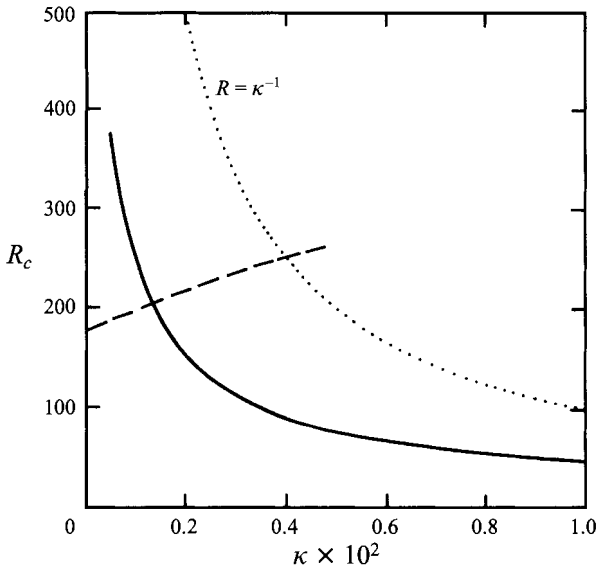

FIGURE 1. Variation of the critical Reynolds number with the streamline curvature κ in the false-flow problem. (Solid line: the new stability; dashed line: the cross-flow instability; dotted line: the condition $R = \kappa^{-1}$.)

The main aim in this section is to clarify the effects of streamline curvature on the instability of the false flow where the curvature is assumed to be independent of the local Reynolds number. This assumption gives the great advantage that we have a free parameter representing the magnitude of the curvature of flow field and can see variations of stability characteristics with this parameter. In computations here, we restrict our attention to the critical Reynolds number R_c of given flows, because it is the simplest and most useful quantity for evaluation of instability characteristics. Variations of R_c with the streamline curvature κ will provide us with important information about instability mechanism in the false flow and, in fact, in the real rotating-disk flow. Figure 1 shows the variation of R_c with κ. The dotted line denotes the relation $R = \kappa^{-1}$, on which the solutions give the critical values of the real flow on a rotating disk. The dashed line denotes the critical curve of the familiar cross-flow (C-F) instability. The point at $\kappa = 0$ on this curve corresponds to the critical value $R_c = 177$ obtained from the Orr–Sommerfeld equation, where the effect of curvature is ignored, while the intersection of this curve with the dotted line gives the critical Reynolds number $R_c = 250.1$ for the real curved flow. These results show a stabilizing effect of the curvature on the C-F instability. On the other hand, the solid line given indicates the existence of another instability in this flow, whose κ-dependency is very different from that of the C-F instability; that is, the critical Reynolds number sharply rises towards infinity as κ decreases to zero. Extended computations to larger values of κ also show that this critical curve intersects with line $R = \kappa^{-1}$ at a Reynolds number much less than 100. From the above study on the false flow, therefore, we may deduce that a new instability entirely different from the cross-flow type will appear in the real rotating-disk flow at a considerably lower Reynolds number. It should be noted, however, that the system of ordinary differential equations given in this paper is an approximate one of substantially same level as the parallel-flow approximation and so is in principle valid for large Reynolds number, although there is no reliable estimation of the lower limit for validity. This suggests that the new critical Reynolds number thus

obtained for the real flow may be outside the range of validity in the present computation.

More detailed investigation of the numerical results for the new instability indicates that the critical curve approximately satisfies the relation $R_c \sim \kappa^{-1/2}$, leading to the deduction that this instability may be of the centrifugal type. As is well known, the stability limit of two-dimensional boundary layers along a concave wall with the curvature κ_w is represented by a critical value G_c of the Görtler number defined by $G = \kappa_w^{1/2} R$, so that variation of the critical Reynolds number with the wall curvature is given by $R_c = G_c/\kappa_w^{1/2}$. This is of the same form as the present relation between the critical Reynolds number and the streamline curvature, as seen above. Since the critical Reynolds number increases to infinity as κ tends to zero, our new instability may be considered to disappear at the limit of no curvature. This is the reason why no instability, besides the C-F one, can be obtained from the Orr–Sommerfeld equation where the curvature terms are ignored (see Mack 1984; Itoh 1985). It is also very important to note that the rotation of flow field, which is inherent in the present problem, is not essential to this instability, because the principal curvature term appears and plays the same role even in the stability equations for the case of no rotation, as seen in (2.5); the same kind of instability has been found to occur in three-dimensional boundary layers on a stationary surface (Itoh 1994*b*). All this seems to tell us that this new instability is of the centrifugal type due to the curvature of flow field, and therefore we follow the author's previous work and call it the streamline-curvature (S-C) instability.

Having confirmed the appearance of the S-C instability in the false flow, we now turn to the problem of the real flow on a rotating disk, whose stability characteristics can be extracted from solutions of the generalized problem given above by imposing the condition $R = \kappa^{-1}$. This will provide information to compare with the existing results of stability computations on the rotating-disk flow. The eigenrelation (2.8), solved subject to the condition of neutral stability, defines a surface in the three-dimensional space (α, β, R), and intersection of this surface with the plane of $R = \text{const.}$ gives a neutral curve on the wavenumber plane. Computational results for the neutral curves are summarized in figure 2, which shows the variation of the wavenumber region of growing disturbances with the Reynolds number. For $R = 200$, which is lower than the critical Reynolds number of C-F instability, the curve indicates the wavenumber region of growing S-C disturbances. For a larger Reynolds number, the instability region of C-F disturbances appears and becomes larger as R increases, while the region of S-C disturbances seems to slightly decrease with R. For $R = 400$ and 600, the two regions are connected, resulting in a single neutral curve, although their original contours seem to be roughly maintained. In this figure, the small open circles indicate the points of stationary disturbances on the neutral curves, and the frequency of non-stationary disturbances is positive on the right-hand side of the line linking these points and negative on the left. We can see that most growing S-C disturbances have positive frequencies. It should also be noted that most of the open circles are on the C-F neutral curves but those on the lower branches for the cases of $R = 400$ and 600 seem to be related to the S-C instability. This suggests that the stationary disturbances associated with the last two open circles in the range of very small wavenumbers may have quite different properties from the well-known stationary C-F disturbances with considerably larger wavenumbers.

For a proper interpretation of our computational results, we may compare the qualitative features of the neutral curves given above with those obtained by Lilly (1966), Balakumar & Malik (1990) and Faller (1991). In spite of different simplifications

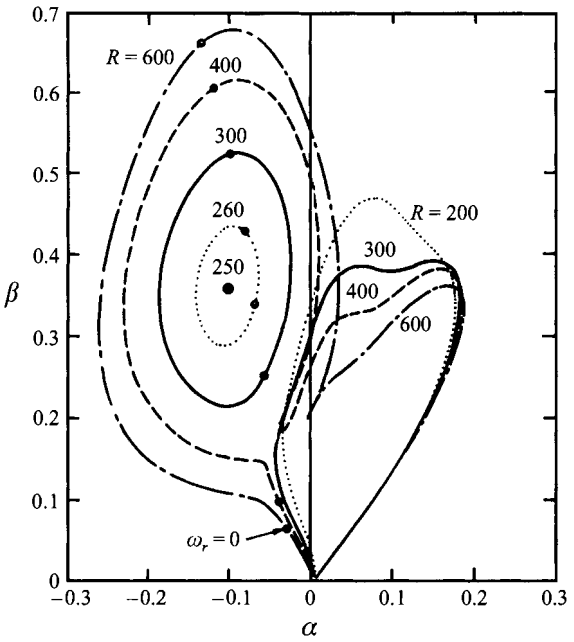

FIGURE 2. Neutral curves on the wavenumber plane for fixed values of the Reynolds number in the real rotating-disk problem.

of the disturbance equations and different methods of presentation, we can find a close resemblance between our new results and the existing ones. First, the neutral curves given in figure 2 are very similar to those of Lilly in having two peaks of the growth rate in the wavenumber plane, indicating the presence of two kinds of instabilities. The present critical Reynolds number 250.1 of C-F instability is not very far from the more accurate value 285.3 obtained by Faller (1991), and the limiting slope of the right-hand branch, i.e. the portion almost independent of Reynolds numbers, of the S-C neutral curves in figure 2 seems to correspond to the critical angle $-35.34°$ reported by Balakumar & Malik (1990). Also, the stationary viscous mode investigated by Malik (1986) and Hall (1986) is likely to be related to the open circles on the lower left-hand branch of the S-C neutral curves in figure 2 (see also Faller 1991). From this close correspondence we can draw the somewhat surprising but quite reasonable conclusion that the S-C instability found in this paper is identical with that called the 'parallel' or 'type 2' instability in the above literature. The most important point to be emphasized is that the present analysis based on a very simple model of disturbance equations has properly described most of the fundamental features of stability characteristics that were revealed by studies using more accurate and much more complicated equations.

4. Attachment-line flow and disturbance equations

The stability analysis of the rotating-disk flow given in the previous sections has confirmed the existence of the streamline-curvature instability, because it is identical with the classical instability of rotating flows that is well known in the field of atmospheric science and has been observed in several experiments. As predicted in the author's previous studies (Itoh 1994*b*, 1995), this instability can occur even in steady boundary layers on swept wings, although no experimental confirmation has yet been obtained. Since the theory predicts the appearance of the S-C instability in an

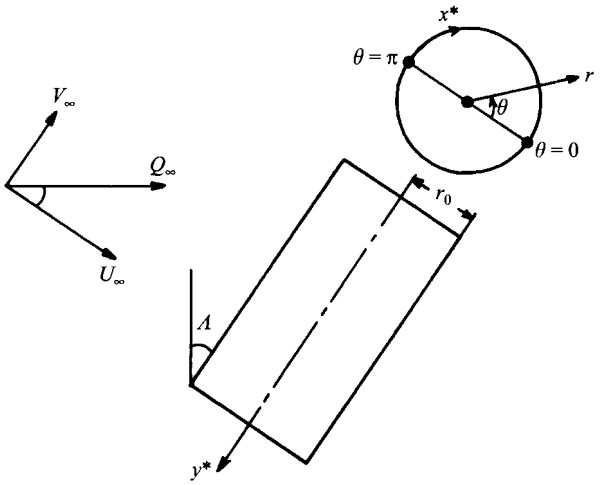

FIGURE 3. Flow situation and coordinate system of the attachment-line problem.

upstream region of the boundary layer on a swept wing, it is of particular interest to examine the possibility of multiple instabilities of the three-dimensional flow near the leading edge of a wing, as done in the problem of rotating-disk flow. In the remainder of this paper, therefore, we tackle the problem of attachment-line flow with the main aims of revealing multiple stability characteristics of this basic flow and of their relations to those of the downstream boundary layer.

For simplicity, we consider the flow around a yawed circular cylinder placed in a uniform flow of a constant velocity Q_∞, as shown in figure 3, where Λ and r_0 denote the sweep angle and radius, respectively, of the cylinder. Let (r, θ, y^*) be cylindrical polar coordinates, t^* time, (v_r, v_θ, v_y) velocity components, p^* pressure, ρ density and ν kinematic viscosity. This coordinate system is different from that used in §2, because it is more convenient for simple expression of the flow situation concerned. Then the external potential flow in the $-\theta$-direction along the cylinder surface is given by a sinusoidal function of θ, which may be expanded in the power series

$$U_E = 2Q_\infty \cos\Lambda \left\{ \frac{x^*}{r_0} - \frac{1}{3!}\left(\frac{x^*}{r_0}\right)^3 + \frac{1}{5!}\left(\frac{x^*}{r_0}\right)^5 - \ldots \right\}, \tag{4.1}$$

where $x^* = r_0(\pi - \theta)$. Since our attention here is directed to a narrow region near the leading edge, we introduce a lengthscale L denoting the extent of the flow region concerned and make the surface distance x^* dimensionless as $X = x^*/L$. If x^* is replaced with X and the ratio $\epsilon_1 = L/r_0$ is assumed to be small, (4.1) may be approximated only by the leading term with neglect of the $O(\epsilon_1^3)$ terms. Then the velocity components of the external flow in the $-\theta$- and $-y^*$-directions are written in the form

$$U_E = 2\epsilon_1 U_\infty X, \quad V_E = V_\infty, \tag{4.2}$$

where $U_\infty = Q_\infty \cos\Lambda$ and $V_\infty = Q_\infty \sin\Lambda$. In this region near the leading edge, the boundary-layer thickness is defined by $\delta = (\nu x^*/U_E)^{1/2}$ and becomes constant, and the viscous flow along the surface has the well-known velocity distributions of the form

$$\bar{u} = U_E F'(\zeta), \quad \bar{v} = V_E G(\zeta), \quad \bar{w} = -\frac{\nu}{\delta} F(\zeta), \tag{4.3}$$

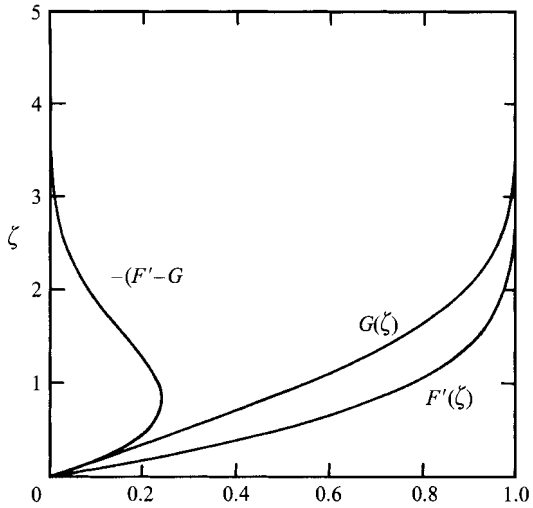

FIGURE 4. Velocity distributions of the attachment-line flow.

where $(\bar{u}, \bar{v}, \bar{w})$ denote the velocity components in the $(-\theta, -y^*, r)$ directions, respectively, $\zeta \equiv (r-r_0)/\delta$ is the similarity variable and F and G are solutions of the ordinary differential equations

$$\left.\begin{aligned} &F''' + FF'' + 1 - (F')^2 = 0, \quad F(0) = F'(0) = 0, \quad F'(\infty) = 1, \\ &G'' + FG' = 0, \quad G(0) = 0, \quad G(\infty) = 1. \end{aligned}\right\} \tag{4.4}$$

This flow is a member of the Falkner–Skan–Cooke family of velocity distributions and includes a cross-flow velocity component normal to the external potential flow. If $\bar{u}$ and $\bar{v}$ are transformed into the streamwise components $\bar{u}_s$ and the cross-flow component $\bar{v}_s$ and non-dimensionalized with the local velocity $Q_E = (U_E^2 + V_E^2)^{1/2}$ of the external flow, we have

$$\frac{\bar{u}_s}{Q_E} = F'(\zeta) + \frac{\gamma^2}{1+\gamma^2}\{G(\zeta) - F'(\zeta)\}, \quad \frac{\bar{v}_s}{Q_E} = \frac{\gamma}{1+\gamma^2}\{G(\zeta) - F'(\zeta)\}, \tag{4.5}$$

where $\gamma \equiv V_E/U_E$ represents the inclination of external streamlines from the x^*-axis. Figure 4 gives distributions of $F'(\zeta)$, $G(\zeta)$ and $G(\zeta) - F'(\zeta)$ to show that the cross-flow distribution has a point of inflexion, which is known to work well on the instability of the flow. The second equation in (4.5) indicates that the magnitude of the cross-flow depends on the streamline inclination and becomes very small as γ tends to zero or infinity. The cross-flow is maximum at $\gamma = 1$ but even then it is generally small in comparison with the streamwise component. Another important property of this flow is that the magnitude of the velocity component $\bar{w}$ in (4.3) becomes large without limit as the distance ζ from the wall increases, because the function $F(\zeta)$ approaches ζ + const. for larger values of ζ. This is a great difference from the case of rotating-disk flow, whose velocity component in the vertical direction vanishes far away from the wall.

We now derive the equations governing small disturbances superimposed on the above basic flow. Since the present coordinate system and fundamental properties of the basic flow are quite different from those given in the previous sections, it may be appropriate to begin with an exact expression of the disturbance equations. First, we introduce two small parameters defined by $\kappa_w = \delta/r_0$ and $\epsilon_0 = \delta/L$: the former denotes

non-dimensional curvature of the wall and the latter acts as a substitute for ϵ_1 through the relation $\epsilon_0 = \kappa_w/\epsilon_1$. We note that there is no explicit parameter denoting the curvature of external streamlines, because the coordinate system here is independent of the direction of the local flows. Next, all other quantities are made dimensionless with a reference velocity Q_0 and the boundary-layer thickness δ as

$$\left.\begin{aligned} &\frac{r_0(\pi-\theta)}{\delta} = x, \quad \frac{y^*}{\delta} = -y, \quad \frac{r-r_0}{\delta} = \zeta, \quad \frac{Q_0 t^*}{\delta} = t, \\ &\frac{v_\theta}{Q_0} = -U-u_1, \quad \frac{v_y}{Q_0} = -V-v_1, \quad \frac{v_r}{Q_0} = \frac{W}{R}+w_1, \quad \frac{p^*}{\rho Q_0^2} = P+p_1, \end{aligned}\right\} \tag{4.6}$$

where (u_1, v_1, w_1, p_1) denote the small disturbance superimposed on the basic flow $(U, V, R^{-1}W, P)$, $R \equiv Q_0\delta/\nu$ being the Reynolds number, and negative signs in front of y, V and v_1 have been introduced to yield the right-hand system of coordinates. If we substitute (4.6) into the Navier–Stokes and continuity equations, subtract the basic-flow parts and neglect coupling terms of the small disturbance, then linearized disturbance equations are obtained in the form

$$\left[\frac{1}{R}\left(\nabla^2-\frac{\kappa_w^2}{h^2}\right)-\frac{\partial}{\partial t}-\frac{U}{h}\frac{\partial}{\partial x}-V\frac{\partial}{\partial y}-\frac{W}{R}\mathrm{D}-\frac{\epsilon_0}{h}\frac{\partial U}{\partial X}-\frac{\kappa_w}{Rh}W\right]u_1$$
$$+\left[\frac{2\kappa_w}{Rh^2}\frac{\partial}{\partial x}-\mathrm{D}U-\frac{\kappa_w}{h}U\right]w_1-\frac{1}{h}\frac{\partial p_1}{\partial x}=0, \tag{4.7a}$$

$$\left[\frac{1}{R}\nabla^2-\frac{\partial}{\partial t}-\frac{U}{h}\frac{\partial}{\partial x}-V\frac{\partial}{\partial y}-\frac{W}{R}\mathrm{D}\right]v_1-\frac{\epsilon_0}{h}\frac{\partial V}{\partial X}u_1-\mathrm{D}V w_1-\frac{\partial p_1}{\partial y}=0, \tag{4.7b}$$

$$\left[\frac{1}{R}\left(\nabla^2-\frac{\kappa_w^2}{h^2}\right)-\frac{\partial}{\partial t}-\frac{U}{h}\frac{\partial}{\partial x}-V\frac{\partial}{\partial y}-\frac{W}{R}\mathrm{D}-\frac{\mathrm{D}W}{R}\right]w_1$$
$$+\left[-\frac{2\kappa_w}{Rh^2}\frac{\partial}{\partial x}+\frac{2\kappa_w}{h}U-\frac{\epsilon_0}{Rh}\frac{\partial W}{\partial X}\right]u_1-\mathrm{D}p_1=0, \tag{4.7c}$$

$$\frac{1}{h}\frac{\partial u_1}{\partial x}+\frac{\partial v_1}{\partial y}+\left(\mathrm{D}+\frac{\kappa_w}{h}\right)w_1=0, \tag{4.7d}$$

where $h = 1+\kappa_w\zeta$, $\mathrm{D} = \partial/\partial\zeta$ and $\nabla^2 = \mathrm{D}^2+\kappa_w h^{-1}\mathrm{D}+h^{-2}\partial^2/\partial x^2+\partial^2/\partial y^2$.

The above form of the disturbance equations does not include explicit terms for the streamline curvature, which may be absorbed into non-parallel terms of the basic boundary-layer flow. Our basic flow is a function of X and ζ and its X-dependence yields the curvature of the flow field, where X is a large-scale variable defined by $X = \epsilon_0 x$. However, we learn from the formulation given in §2 that the curvature appears in the leading terms of the coefficients of u in the simultaneous equation (2.6*b*), which was obtained by eliminating v and p from (2.5). It is therefore appropriate for identification of the curvature term to eliminate the pressure p_1 and the spanwise velocity component v_1 from (4.7). We may then seek a solution of the equations in the wavy form

$$u_1 = u(\zeta; X)\,\mathrm{e}^{\mathrm{i}\Theta}, \quad \Theta = \int^{\epsilon_0 x}\frac{\alpha(X)}{\epsilon_0}\mathrm{d}X+\beta y-\omega t, \tag{4.8}$$

together with corresponding expressions for v_1, w_1 and p_1. Here α and β are real and

denote wavenumbers in the x- and y-directions and ω is complex, the real and imaginary parts denoting frequency and temporal growth rate of disturbances, respectively. The dependence of u and α on the large-scale variable X comes from that of the basic flow. This yields the simultaneous equations for u and w as

$$\left[(\alpha^2+\beta^2)\left\{\frac{1}{R}(\mathrm{D}^2-\alpha^2-\beta^2)+\mathrm{i}(\omega-\alpha U-\beta V)-\frac{W}{R}\mathrm{D}-\epsilon_0\left(U\frac{\partial}{\partial X}+\frac{\partial U}{\partial X}\right)\right\}\right.$$

$$+\epsilon_0\left\{(\omega-\alpha U-\beta V)\left(2\alpha\frac{\partial}{\partial X}+\frac{\mathrm{d}\alpha}{\mathrm{d}X}\right)-2\alpha\frac{\mathrm{d}\alpha}{\mathrm{d}X}U\right\}$$

$$\left.+\mathrm{i}\kappa_w\zeta\{\alpha(\alpha^2+\beta^2)U-2\alpha^2(\omega-\alpha U-\beta V)\}+O\left(\epsilon_0,\frac{1}{R},\kappa_w\right)^2\right]u$$

$$-\left[\mathrm{i}\alpha\left\{\frac{1}{R}(\mathrm{D}^2-\alpha^2-\beta^2)+\mathrm{i}(\omega-\alpha U-\beta V)-\frac{W}{R}\mathrm{D}-\epsilon_0 U\frac{\partial}{\partial X}\right\}\mathrm{D}+\beta(\beta U'-\alpha V')\right.$$

$$+\mathrm{i}\epsilon_0\left\{(\omega-\alpha U-\beta V)\frac{\partial}{\partial X}\mathrm{D}-\left(\alpha\frac{\partial U}{\partial X}+\frac{\mathrm{d}\alpha}{\mathrm{d}X}U+\beta\frac{\partial V}{\partial X}\right)\mathrm{D}+\beta\left(V'\frac{\partial}{\partial X}+\frac{\partial V'}{\partial X}\right)\right\}$$

$$-\kappa_w\{\alpha(\omega-\alpha U-\beta V)(1-\zeta\mathrm{D})-\beta(\beta U+\alpha\zeta V')+\alpha^2\zeta U\mathrm{D}\}$$

$$\left.+O\left(\epsilon_0,\frac{1}{R},\kappa_w\right)^2\right]w=0, \tag{4.9a}$$

$$\left[\left\{\frac{1}{R}(\mathrm{D}^2-\alpha^2-\beta^2)+\mathrm{i}(\omega-\alpha U-\beta V)-\frac{W}{R}\mathrm{D}-\frac{W'}{R}-\epsilon_0 U\frac{\partial}{\partial X}\right\}\right.$$

$$\times(\mathrm{D}^2-\alpha^2-\beta^2)+\mathrm{i}(\alpha U''+\beta V'')$$

$$-\epsilon_0\left\{(\omega-\alpha U-\beta V)\left(2\alpha\frac{\partial}{\partial X}+\frac{\mathrm{d}\alpha}{\mathrm{d}X}\right)-2\alpha\left(\alpha\frac{\partial U}{\partial X}+\beta\frac{\partial V}{\partial X}\right)\right.$$

$$\left.-\left(\frac{\partial U'}{\partial X}\mathrm{D}+\frac{\partial U''}{\partial X}+U''\frac{\partial}{\partial X}\right)\right\}$$

$$+\mathrm{i}\kappa_w\{(\omega-\alpha U-\beta V)(\mathrm{D}+2\alpha^2\zeta)-(\alpha U'+\beta V')+2\alpha(U\mathrm{D}+U')$$

$$\left.+\alpha\zeta U(\mathrm{D}^2-\alpha^2-\beta^2)-\alpha\zeta U''\}+O\left(\epsilon_0,\frac{1}{R},\kappa_w\right)^2\right]w$$

$$+\left[2\mathrm{i}\epsilon_0\left\{\left(\alpha\frac{\partial U}{\partial X}+\beta\frac{\partial V}{\partial X}\right)\mathrm{D}+\left(\alpha\frac{\partial U'}{\partial X}+\beta\frac{\partial V'}{\partial X}\right)\right\}\right.$$

$$\left.+2\kappa_w\{\alpha(\omega-\alpha U-\beta V)-(\alpha^2+\beta^2)U\}+O\left(\epsilon_0,\frac{1}{R},\kappa_w\right)^2\right]u=0, \tag{4.9b}$$

where the prime denotes differentiation with respect to ζ. These equations are of the partial differential type with respect to ζ and X, but we expect that an appropriate method of order estimation can reduce them to a simple system of ordinary differential

equations, which enables us to evaluate the local stability characteristics of the given flow with solutions of an eigenvalue problem. The simplification will be given in the next section.

5. Reduction to an eigenvalue problem

In this section, we examine the balance of the principal terms in the disturbance equations (4.9) for different values of sweep angle and different modes of disturbances, and then simplify the exact partial-differential equations to an approximate system of ordinary differential equations by retaining the most important terms only. Before doing this, we see how (4.9) includes effects of the streamline curvature, because there is no explicit term corresponding to the curvature term in (2.6). Consider the coefficients of u in (4.9*b*), where the differential terms $\partial U/\partial X$ and $\partial U'/\partial X$ may be replaced with U/X and U'/X, respectively, and $\partial V/\partial X = \partial V'/\partial X = 0$, because U is proportional to X and V is independent of X in this problem. If the relation $\epsilon_0/X = ((1+\gamma^2)^{1/2}/R)\,(Q_0/Q_E)$ is used in addition, then the leading terms proportional to ϵ_0 can be rewritten as

$$2\mathrm{i}\epsilon_0\left\{\left(\alpha\frac{\partial U}{\partial X}+\beta\frac{\partial V}{\partial X}\right)\mathrm{D}+\left(\alpha\frac{\partial U'}{\partial X}+\beta\frac{\partial V'}{\partial X}\right)\right\}u = \frac{2\mathrm{i}\alpha(1+\gamma^2)^{1/2}}{R}\left(\frac{Q_0}{Q_E}\right)(U\mathrm{D}+U')\,u. \quad (5.1)$$

While the reference velocity Q_0 is not yet specified, the curvature of the external streamlines is obtained from the inclination γ and its derivative with respect to X and is written in the dimensionless form

$$\kappa_s = \frac{\gamma}{R(1+\gamma^2)}\frac{Q_0}{Q_E}, \quad (5.2)$$

where the reference length is the boundary-layer thickness δ. It is therefore possible to eliminate R from (5.1) by the use of (5.2), resulting in u-terms proportional to the curvature κ_s. If we consider disturbances of the longitudinal-vortex type and transform x and y into the coordinates ξ and η parallel and perpendicular to the streamlines, we find that the corresponding u-terms in (4.9*b*) can be rewritten approximately in the same form as the curvature terms in the previous formulation (2.6). These terms may be expected to induce a centrifugal-type streamline-curvature instability even in the present problem.

To simplify the disturbance equations (4.9), we consider the case $\epsilon_0 = \epsilon_1 = \kappa_w^{1/2}$ and assume that the cross-flow component of the basic flow has a magnitude of $O(\epsilon_0^{1/2})$. The assumption of small cross-flow may be mathematically justified only if the streamline inclination is either very small or very large, such as $\gamma \approx O(\epsilon_0^{1/2})$ or $\gamma^{-1} \sim O(\epsilon_0^{1/2})$, but here we apply it to all values of γ for the physical reason that the cross-flow component is generally smaller than the streamwise component, as shown in figure 4. Under these conditions, we examine the fundamental balance of various terms in the disturbance equations. Let us begin with the case where the sweep angle Λ of the cylinder is so small as to be of $O(\epsilon_0)$. If we take $V_E = Q_\infty \sin\Lambda$ as the reference velocity Q_0, the basic flow in dimensionless form has the spanwise component V of $O(1)$ and the streamwise component U of the same order, and R^{-1} becomes of $O(\epsilon_0)$, because substitution of $\delta = (\nu r_0/2U_\infty)^{1/2}$ into the definition of the Reynolds number leads to the general relation

$$\frac{1}{R} = \frac{2\kappa_w Q_\infty \cos\Lambda}{Q_0}. \quad (5.3)$$

If disturbances are of the longitudinal-vortex type, their wavenumber vectors are nearly perpendicular to the basic flow, and then α and β are of $O(1)$ but the inner product $\alpha U+\beta V$ yields a cross-flow component, which is assumed to be of $O(\epsilon_0^{1/2})$ here. Since ω has the same magnitude as the inner product, we may assume the orders of magnitude as

$$U, V, W, \alpha, \beta, u \sim O(1); \quad \alpha U+\beta V, \omega, w \sim O(\epsilon_0^{1/2}); \quad R^{-1} \sim O(\epsilon_0), \tag{5.4}$$

and then the leading-order approximation of (4.9) is given by

$$[\mathrm{i}(\alpha^2+\beta^2)(\omega-\alpha U-\beta V)+O(\epsilon_0)]u+[-\beta(\beta U'-\alpha V')+O(\epsilon_0^{1/2})]w=0, \tag{5.5a}$$

$$[\mathrm{i}(\omega-\alpha U-\beta V)(\mathrm{D}^2-\alpha^2-\beta^2)+\mathrm{i}(\alpha U''+\beta V'')+O(\epsilon_0)]w + \left[\epsilon_0\frac{2\mathrm{i}\alpha}{X}(U\mathrm{D}+U')+O(\epsilon_0^2)\right]u=0. \tag{5.5b}$$

Next we consider the case of normally large sweep angle, so that U_E is much smaller than V_E. If the reference velocity is again chosen as $Q_0 = V_E$, the velocity component V is of $O(1)$ but the streamwise component U is of $O(\epsilon_0)$, and the wavenumbers α and β of the longitudinal disturbances are of $O(1)$ and of $O(\epsilon_0)$, respectively. If we apply the above method of order estimation to this case, we have

$$V, W, \alpha, u, w \sim O(1); \quad U, \beta, \omega \sim O(\epsilon_0); \quad R^{-1} \sim O(\epsilon_0^2), \tag{5.6}$$

and then the lowest-order equations are obtained in the form (5.5) with a few terms neglected, indicating that the case of small sweep angle gives the most general form of approximate equations. Finally, we consider disturbances that are not of the longitudinal-vortex type, so that all of the velocity components and the wavenumbers may be assumed to be order unity for the sweep angle of $O(\epsilon_0)$. Then the leading-order terms become

$$[\mathrm{i}(\alpha^2+\beta^2)(\omega-\alpha U-\beta V)+O(\epsilon_0)]u + [\alpha(\omega-\alpha U-\beta V)\mathrm{D}-\beta(\beta U'-\alpha V')+O(\epsilon_0)]w=0, \tag{5.7a}$$

$$[\mathrm{i}(\omega-\alpha U-\beta V)(\mathrm{D}^2-\alpha^2-\beta^2)+\mathrm{i}(\alpha U''+\beta V'')+O(\epsilon_0)]w+[O(\epsilon_0)]u=0, \tag{5.7b}$$

for small sweep angle, but the terms proportional to U in (5.7) are absorbed into the smaller-order terms for large sweep angle.

As seen above, the leading-order terms in the disturbance equations vary with the conditions of the basic flow and types of the disturbance concerned. The smaller-order terms neglected in the above, however, include some important terms associated with the viscosity and non-parallelism of the flow. As stated in §2, the viscous term $R^{-1}(\mathrm{D}^2-\alpha^2-\beta^2)$ plays certain fundamental roles in the critical and wall layers, where disturbances vary very sharply. Furthermore, the author's previous studies (Itoh 1994*a*, *b*) have shown that the term $R^{-1}W$ in (4.9) (corresponding to $R^{-1}\hat{W}$ in the quoted papers) represents the most important effects of non-parallel boundary-layer flows and seriously affects the decaying behaviour of disturbances in the external region away from the wall, because the velocity component W increases in proportion to the distance ζ there. This is a great difference between the boundary-layer-flow problem discussed here and the rotating-flow problem studied in the previous sections. Now we wish to construct a simple system of ordinary differential equations applicable to all the basic-flow conditions and the disturbance modes concerned. This is done by retaining all the leading terms given in (5.5) and (5.7) together with the viscous and non-parallel terms discussed above. Then, we replace, for convenience of notation, the

reference velocity used so far with the local velocity $Q_E = (U_E^2 + V_E^2)^{1/2}$ of the external flow. Then the approximate disturbance equations are written in the form

$$\left[(\alpha^2+\beta^2)\left\{\frac{1}{R}(\mathrm{D}^2-\alpha^2-\beta^2)+\mathrm{i}(\omega-\alpha U-\beta V)-\frac{W}{R}\mathrm{D}\right\}\right]u$$
$$-\left[\mathrm{i}\alpha\left\{\frac{1}{R}(\mathrm{D}^2-\alpha^2-\beta^2)+\mathrm{i}(\omega-\alpha U-\beta V)-\frac{W}{R}\mathrm{D}\right\}\mathrm{D}+\beta(\beta U'-\alpha V')\right]w=0, \quad (5.8a)$$

$$\left[\left\{\frac{1}{R}(\mathrm{D}^2-\alpha^2-\beta^2)+\mathrm{i}(\omega-\alpha U-\beta V)-\frac{W}{R}\mathrm{D}-\frac{W'}{R}\right\}(\mathrm{D}^2-\alpha^2-\beta^2)+\mathrm{i}(\alpha U''+\beta V'')\right]w$$
$$+\frac{2\mathrm{i}\alpha(1+\gamma^2)^{1/2}}{R}(U\mathrm{D}+U')u=0, \quad (5.8b)$$

where $R \equiv Q_E\delta/\nu$ is the Reynolds number based on the local velocity of the external flow, and the velocity components of the basic flow are given by

$$U=\frac{1}{(1+\gamma^2)^{1/2}}F'(\zeta), \quad V=\frac{\gamma}{(1+\gamma^2)^{1/2}}G(\zeta), \quad W=-F(\zeta). \quad (5.9)$$

Thus the present equation system is certainly applicable to the three kinds of instability due to viscosity, cross-flow and streamline curvature and is suitable for our purpose of investigating multiple stability characteristics of the attachment-line flow.

The approximate disturbance equations given above are very similar to those used in Itoh (1994*b*), so that the boundary conditions to be imposed may be obtained through the procedure given there. The results are written in the approximate form

$$u=w=w'=0 \quad \text{at} \quad \zeta=0, \quad (5.10a)$$

$$u'+\rho_1 u-\frac{\mathrm{i}\alpha}{\rho_2^2}(w''+\rho_1 w')=0, \quad (5.10b)$$

$$w''+(\rho_1+\rho_2)w'+\rho_1\rho_2 w-\frac{2\mathrm{i}\alpha\rho_1 U_0(1+\gamma^2)^{1/2}}{(2\rho_1+W_0)(\rho_1+\rho_2)}u=0, \quad (5.10c)$$

$$w'''+(2\rho_1+\rho_2)w''+\rho_1(\rho_1+2\rho_2)w'+\rho_1^2\rho_2 w=0 \quad \text{at} \quad \zeta=\zeta_e, \quad (5.10d)$$

where $\rho_1=-\frac{1}{2}W_0+(\frac{1}{4}W_0^2+\alpha^2+\beta^2-\mathrm{i}\omega R+\mathrm{i}\alpha RU_0+\mathrm{i}\beta RV_0)^{1/2}$, $\rho_2=(\alpha^2+\beta^2)^{1/2}$, and the subscript 0 denotes the value at the boundary-layer edge ζ_e. These conditions are not exact but can provide sufficient accuracy if the boundary-layer edge is taken large, i.e. $\zeta_e=10$ (Itoh 1994*a*). Together with the above boundary conditions, the homogeneous equations (5.8) pose an eigenvalue problem to determine the complex frequency ω as a function of the wavenumbers α and β, the Reynolds number R and the flow parameter γ as

$$\omega=\omega(\alpha,\beta,R;\gamma), \quad (5.11)$$

whose real part ω_r denotes frequency and imaginary part ω_i temporal growth rate of the disturbance. Solution of the eigenvalue problem and determination of the critical points for given values of γ are done with the numerical method described in §2.

6. Multiple instabilities of the attachment-line flow

The velocity distribution of the attachment-line flow is obtained by putting the pressure parameter m equal to 1.0 in the Falkner–Skan–Cooke flow. Critical Reynolds numbers of the cross-flow instability in this flow have been obtained in Itoh (1991),

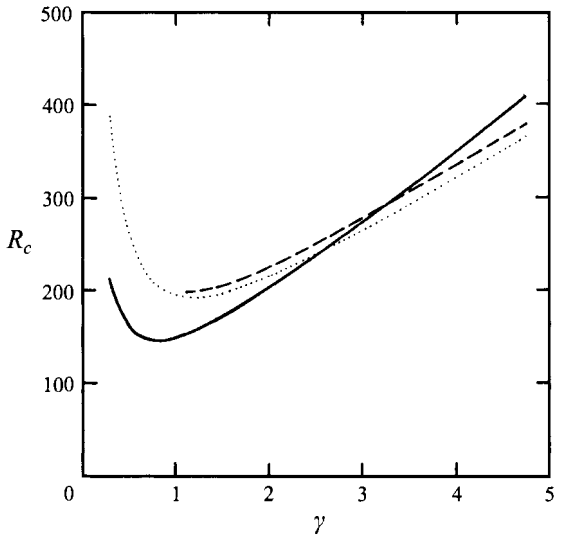

FIGURE 5. Critical Reynolds numbers plotted against γ. (Solid line: the new instability; dashed line: the cross-flow instability obtained from (5.8); dotted line: the cross-flow instability obtained from (5.8) with neglect of the curvature terms.)

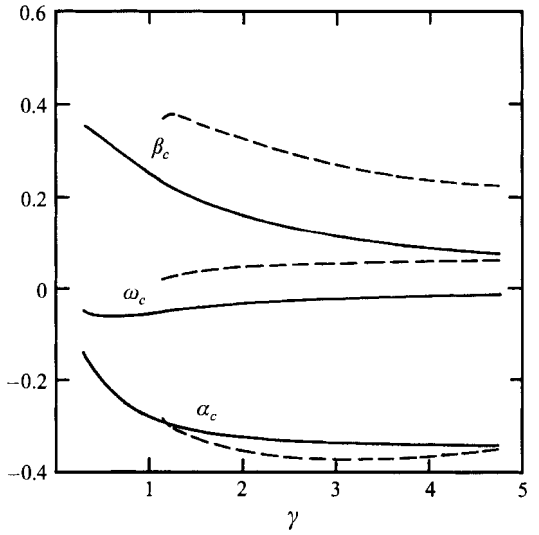

FIGURE 6. Variations of wavenumbers and frequency of disturbances along the critical curves given in figure 5. (Solid line: the new mode; dashed line: the cross-flow mode.)

where the Orr–Sommerfeld equation was used with neglect of the streamline-curvature terms. In the present paper, therefore, we begin with the simpler equations, ignore the u-terms in (5.8b) and solve the corresponding eigenvalue problem for critical Reynolds numbers of the cross-flow instability in the attachment-line flow. The results are shown by the dotted line in figure 5, where values of R_c are plotted against the inclination γ of external streamlines to the chordwise direction x. The critical curve has a minimum at $\gamma \doteqdot 1.2$ and rises for larger and smaller values of γ. If we use (5.8) without modification, the critical curve for the cross-flow instability shifts to the dashed line, which however disappears for γ less than 1.2 and instead a new critical curve is

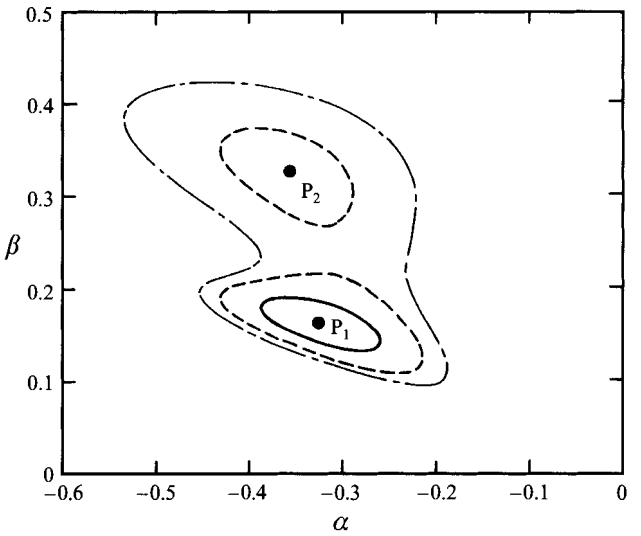

FIGURE 7. Neutral stability curves for fixed values of Reynolds number at $\gamma = 2.0$. (Solid line: $R = 210$; dashed line: $R = 230$; chain-dotted line: $R = 250$; P_1: $R = 201$; P_2: $R = 225$.)

obtained in the whole range of γ, as shown by the solid line in figure 5. The new curve has a similar shape and is distinctly lower than the dashed line in the range of $\gamma < 3.3$, although the cross-flow curve gives the lowest critical values for larger values of γ. These computations indicate that two kinds of instabilities are possible in the attachment-line flow. Of particular importance is that the new instability can be obtained from the disturbance equations (5.8) including the curvature terms in (5.8*b*), but not from the Orr–Sommerfeld equation. This situation is very similar to the cases of rotating-disk flow and of downstream boundary-layer flows (Itoh 1995) and suggests that the new critical curve may belong to the streamline-curvature instability.

Comparisons of wavenumbers and frequency of the critical disturbances along the two critical curves are shown in figure 6, where we can see quite large differences between the solid and dashed lines, in particular for the spanwise wavenumber and the frequency. The cross-flow instability gives larger values of the wavenumber than those of the new instability, and the frequency curves show different signs of ω_c, which indicate opposite directions of propagation of the two kinds of disturbances. These differences in disturbance properties are very similar to the differences between the C-F and S-C disturbances in the Falkner–Skan–Cooke flow revealed by Itoh (1994*b*). To see the wavenumber regions of the two kinds of disturbances, we fixed the value of γ at 2.0 and drew neutral stability curves on the wavenumber plane (α, β) for Reynolds numbers slightly larger than the critical value. In figure 7, the wavenumber components inside each curve have positive growth rates at the corresponding Reynolds number. From these curves, we can imagine the rough shape of the neutral stability surface in the three-dimensional space with the coordinates (α, β, R) and find that the surface has two downward peaks; the higher one is related to the cross-flow instability, while the lower gives the critical Reynolds number at $\gamma = 2.0$ on the solid line in figure 5. This feature of the neutral surface bears a close resemblance to that of the rotating-disk flow, for which the neutral curves are given in figure 2, showing that both the C-F and S-C modes appear competitively. Another comparison is made in figure 8, which presents amplitude and phase distributions of the two critical disturbances at $\gamma = 2.0$ on the solid and dashed lines in figure 5. Only the velocity component in the direction

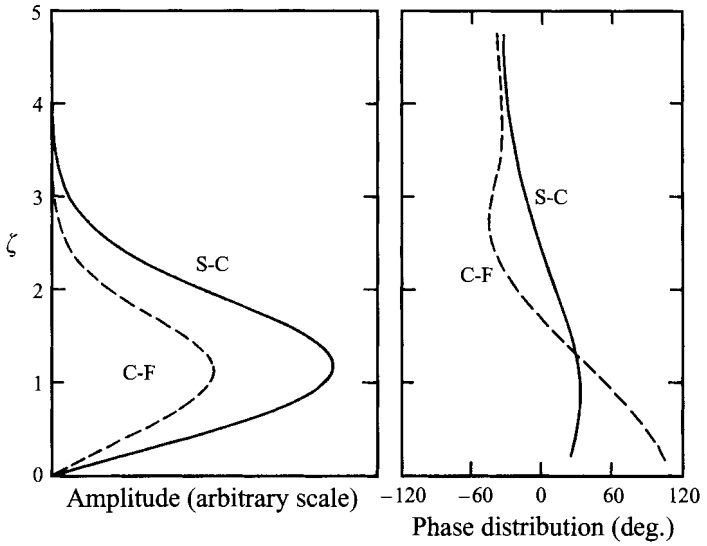

FIGURE 8. Amplitude and phase distributions of the velocity component in the direction of the external streamline of the critical disturbances at $\gamma = 2.0$. (Solid line: the new mode; dashed line: the cross-flow mode.)

of the external streamline is presented here, because the others are one order of magnitude smaller. These distributions also bear a striking resemblance to those of the C-F and S-C disturbances shown in Itoh (1994*b*). Figures 6–8 have great similarities to the corresponding figures presented in the previous studies on the Falkner–Skan–Cooke and rotating-disk flows, and therefore we may conclude that the critical curve denoted by the solid line in figure 5 must belong to the streamline-curvature instability, as deduced earlier.

The results given in figure 5 indicate that the C-F instability gives lower critical Reynolds numbers than the S-C instability only for quite large values of the streamline inclination γ. Since there is larger inclination of streamlines in the region closer to the attachment line, it is interesting to see how the critical curve of the C-F instability behaves as γ increases further, and so additional computations are shown in figure 9, where critical quantities are plotted against γ^{-1}. Important findings are that increase of the critical Reynolds number becomes saturated as γ^{-1} decreases, R_c approaching a constant at $\gamma^{-1} = 0$, and that the wavenumber α_c of the critical disturbances tends to zero with the decrease in γ^{-1}, so that the wavenumber vector becomes parallel to the attachment line. Hall, Malik & Poll (1984) have considered this particular mode of disturbances and succeeded in deriving exact disturbance equations of the ordinary differential form, which are equivalent to those obtained by putting $\alpha = 0$ in our disturbance equations (5.8) and adding a smaller-order term $-2\beta^2 R^{-1} F' u$ to the left-hand side of (5.8*a*). In this particular case, the equation system becomes independent of the basic-flow parameter γ and gives the critical values $R_c = 583.1$, $\beta_c = 0.288$ and $\omega_c = 0.111$. Comparison of these values with figure 9 shows that the critical state obtained by Hall *et al.* corresponds to the limit for $\gamma^{-1} \to 0$ of the critical curve of the C-F instability, which is dominant in the region very close to the attachment line. This conclusion is very useful for our understanding of a fundamental feature of the attachment-line instability.

As seen above, the critical Reynolds number R_c of the attachment-line flow is a function of the inclination γ of the external streamlines from the chordwise direction.

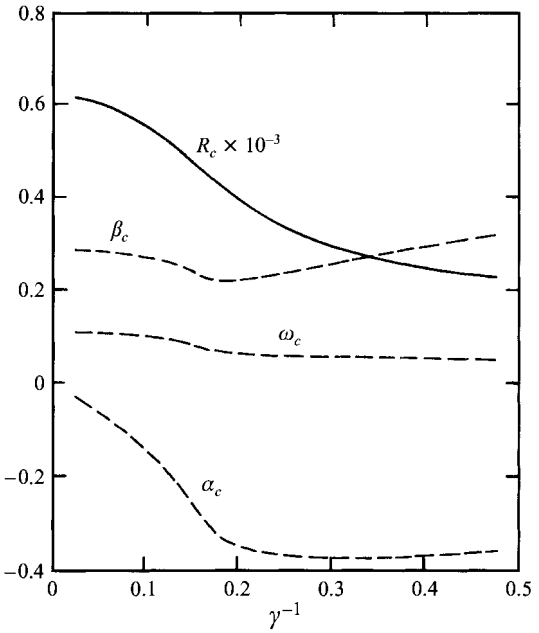

FIGURE 9. Critical values of the cross-flow instability for small values of γ^{-1}.

Since U_E is proportional to X and V_E is constant in the flow near the leading edge of a circular cylinder, the ratio $\gamma = V_E/U_E$ is easily obtained for a given value of the sweep angle Λ of the cylinder as

$$\gamma = \frac{\tan\Lambda}{2\epsilon_1 X} = \frac{\tan\Lambda}{2\pi\hat{X}}, \tag{6.1}$$

where $\hat{X} \equiv \epsilon_1 X/\pi$ denotes the distance made dimensionless with the surface length from the leading edge to the trailing edge. Using this relation, we can find variations of R_c with $\hat{X}$ for fixed values of Λ, and the results are given for sweep angles of $\Lambda = 5°$, 10° and 20° in figure 10. Since the variation of the critical curve $R_c(\hat{X})$ with Λ comes only from stretching the space coordinate, the minimum value of R_c stays the same but its location $\hat{X}_{min}$ is shifted downstream considerably as the sweep angle increases. When the sweep angle is very small, the direction of the external streamlines varies from parallel to the leading edge towards the main stream direction within a very narrow region close to the leading edge, so that the critical Reynolds number decreases sharply to the minimum value, followed by a sharp increase with $\hat{X}$ in this range. If we consider the case that Λ is just zero, on the other hand, the basic flow reduces to the two-dimensional stagnation flow, whose stability characteristics have been studied by many researchers. Linear stability theory shows that this flow is stable for small disturbances of Tollmien–Schlichting waves and also of longitudinal vortices, but there are some reports that certain experiments have detected disturbances of the latter type (see, for instance, Wilson & Gladwell 1978). This discrepancy between theory and experiment may be explained by the present analysis for the three-dimensional flow, because the results suggest the possibility that a minute modification of the two-dimensional stagnation flow to a slightly three-dimensional flow may lead to local instability to longitudinal disturbances as shown in figure 10.

Finally we consider the case of a moderately large sweep angle and investigate the relation between the present critical curves and those of the downstream boundary

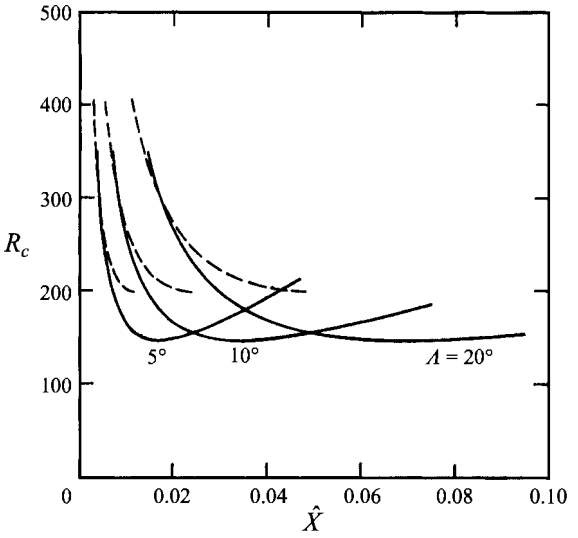

FIGURE 10. Critical Reynolds numbers plotted against the chordwise distance $\hat{X}$ for sweep angles $\Lambda = 5°$, 10° and 20°. (Solid line: the streamline-curvature mode; dashed line: the cross-flow mode.)

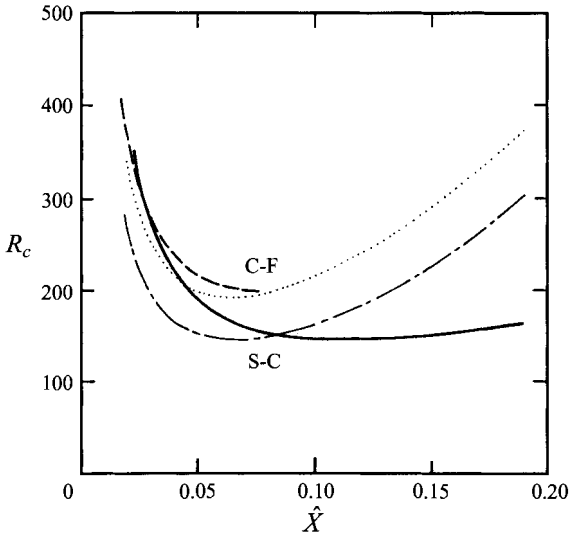

FIGURE 11. Comparison of the critical curves for the case of $\Lambda = 30°$. (Solid line: the streamline-curvature instability of the attachment-line flow; dashed line: the cross-flow instability of the attachment-line flow; chain-dotted line: the streamline-curvature instability of the downstream boundary-layer flow; dotted line: the cross-flow instability of the downstream boundary-layer flow.)

layer. As shown in figure 11, the critical curve of the S-C instability for $\Lambda = 30°$ has a minimum at $\hat{X} \doteqdot 1.1$ and then increases slowly. On the other hand, the critical curves of the downstream boundary-layer flow on a circular cylinder with the same sweep angle have been obtained in Itoh (1996), where the disturbance equations used are based on the coordinates along and normal to the external streamline and include both the wall and streamline curvatures, although the level of approximation is the same as the present equation system. Since the boundary-layer flow is approximated by members of the Falkner–Skan–Cooke velocity family, the critical Reynolds number

depends on the Falkner–Skan parameter m, which approaches to 1.0 as the distance $\hat{X}$ from the leading edge decreases. Comparison of the two series of computational results is made in figure 11, where the S-C and C-F critical curves, denoted by the chain-dotted and fine dotted lines respectively, have been obtained from extended computations of Itoh (1996) to smaller values of $\hat{X}$. We see a fairly good agreement in the qualitative features in the whole range of $\hat{X}$ concerned, in spite of the different treatment of the two curvature terms and the pressure gradient. The previous critical curves for the two instabilities seem to approach the present ones as $\hat{X}$ decreases, which seems to indicate that the previous method of stability calculation is applicable not only to the downstream boundary-layer flow but also to the upstream flow close to the leading edge, at least for the rough estimation of the multiple characteristics in instability of the flows done in the present study.

7. Concluding remarks

A theoretical investigation based on simple models of disturbance equations has been made to reveal multiple characteristics in the instability of rotating-disk flow and attachment-line flow, with particular attention to the possibility of the streamline-curvature instability, which was first predicted in a recent study on general three-dimensional boundary layers (Itoh 1994*b*). In the problem of the rotating-disk flow, the somewhat tricky assumption was introduced of considering a false flow where the curvature of the flow field can vary independently of the local Reynolds number. Constant thickness of the viscous layer and no vertical velocity away from the surface in the basic flow are of great advantage in deriving the simplest model of disturbance equations, which includes an explicit term for the curvature and enables us to determine the critical Reynolds number of the false flow as a function of the curvature parameter κ. In the actual flow on a rotating disk, the curvature is not independent of the local Reynolds number R but is related to it by $R = \kappa^{-1}$, and solutions for this particular case can be sought in general solutions of the above false-flow problem. For the problem of the attachment-line instability, on the other hand, we have considered the flow near the leading edge of a yawed circular cylinder, because of a practical interest in the relation between its instability and the cross-flow and streamline-curvature instabilities of the boundary-layer flow downstream. A model system of disturbance equations was derived through stretching the downstream coordinate near the leading edge and examining the fundamental balance of principal terms in the equations for various sweep angles of the cylinder and for different modes of disturbances. The resulting system consists of the simplest model mentioned above plus the most important non-parallel term associated with the vertical velocity in the boundary-layer flow and is applicable for any value of sweep angle and any mode of disturbances. The two equation systems used in this paper are simple modifications of the parallel-flow approximation with the addition of the principal curvature term and pose eigenvalue problems, which were solved numerically to evaluate critical Reynolds numbers of the flows. This simplicity is suitable for presentation of the effects of streamline curvature separately and for comparing multiple characteristics in the instability of the flows.

Computational results for the rotating-disk problem show the existence of two instabilities induced by different mechanisms. Introduction of the false flow in this study played a fundamental role in clarifying the essential mechanisms of these instabilities. One of them is the well-known cross-flow instability, whose critical Reynolds number is affected only a little by the streamline curvature, indicating that

the effect of cross-flow is essential in the instability mechanism. The other instability is of the streamline-curvature type, because its critical Reynolds number increases infinitely as the curvature decreases to zero. It has also been shown from detailed analysis of computational results that the curvature term remains in the lowest-order approximation of disturbance equations and plays an essential role in this instability.

Further stability analysis of the real flow on a rotating disk has demonstrated the important conclusions that the streamline-curvature instability does appear in real rotating-disk flow and that it is the same one that was called 'parallel' or 'type-2' instability in the classical studies by Lilly (1966) and Faller & Kaylor (1966). This instability has been analysed with more accurate formulations dealing with the real flow subject to the condition $R = \kappa^{-1}$ from the beginning and including complex effects of centrifugal force, Coriolis force and radial variation of the basic flow, which are inherent in rotating flows and appear in the same smaller-order terms as R^{-1} (Faller 1991; Balakumar *et al.* 1991). It should also be noted that the so-called parallel or type-2 instability of rotating flows has been confirmed by several experiments and is well established in the field of atmospheric science.

The most progressive findings of the present study are therefore that overall features of this classical instability are properly described by the very simple disturbance equations consisting of the parallel-flow approximation plus an additional term associated with the curved flow field and that the additional curvature term is in fact responsible for this mode of instability. Thus we may conclude that the present study of the rotating-disk flow has provided reliable evidence for existence of the streamline-curvature instability, which was first predicted for general three-dimensional boundary layers but has not yet been confirmed by experiments on flows without rotation. Since the fundamental activity of the curvature is not restricted to the case of rotating flows, it is quite natural that the boundary layer on a swept wing is sensitive to the same type of instability as the classical instability discussed above.

Computational results for the attachment-line problem show that the streamline-curvature instability is very likely in the flow near the leading edge of a yawed circular cylinder. In this problem, the critical Reynolds number is determined as a function of the basic-flow parameter γ only, which represents the local angle of external streamlines to the chordwise direction normal to the attachment line and is closely related to the curvature of external streamlines. Since γ is a known function of the surface distance $\hat{X}$ from the leading edge and the sweep angle Λ of the cylinder, we can draw the critical curves on the $(\hat{X}, R)$-plane for various values of Λ. For each value of the sweep angle, two kinds of critical curves appear corresponding to the cross-flow and streamline-curvature instabilities, and the S-C critical curve is lower than the C-F one in most of the range of $\hat{X}$ concerned, except for a very narrow region close to the attachment line. This curve has a minimum at a position $\hat{X}_{min}$ and rises very sharply as $\hat{X}$ decreases towards the leading edge but more moderately for larger values of $\hat{X}$ than $\hat{X}_{min}$. For larger values of the surface distance, however, the velocity distribution deviates from that of the attachment-line flow, and therefore the present curve should be replaced with the critical curve for the S-C instability of the downstream boundary layer, which was obtained in the author's previous study on multiple instabilities of three-dimensional boundary layers (Itoh 1996).

Thus we have overall view of the critical conditions along the windward surface of the cylinder. A very narrow region close to the attachment line is governed by the cross-flow instability, but the streamline-curvature instability determines the lowest values of the critical Reynolds number in a much wider region from just downstream of the narrow attachment-line region to a certain station in the downstream boundary layer,

behind which the lowest critical values are again determined by the cross-flow instability. Another interesting conclusion is drawn from the fact that the minimum value of the critical curve is held fixed during variation of the sweep angle. As the sweep angle Λ decreases to zero, the location $\hat{X}_{min}$ of the minimum critical Reynolds number moves towards the leading edge and the distance between the left- and right-hand branches of the critical curve becomes smaller and smaller, resulting in a very sharp fall and rise of the critical value within a narrow range of $\hat{X}$ around $\hat{X}_{min}$. This indicates that stability characteristics of the three-dimensional attachment-line flow in the limit of small sweep angle differ radically from those of the two-dimensional stagnation flow, which is known to be stable to any kind of small disturbance.

The above results have been obtained from solution of the approximate disturbance equations, which were derived without mathematical justification, although most attention was paid to keeping the most important terms in the equations. A more rigorous analysis of the attachment-line instability has been done by Hall *et al.* (1984), who considered a limited disturbance with wavenumber vector parallel to the attachment line. In that case, we can derive an exact system of ordinary differential equations, which are however found to be independent of the streamline inclination γ. Comparative examination indicates that the critical point obtained by Hall *et al.* corresponds to the limit for $\gamma \to \infty$ of the present critical curve of the cross-flow instability appearing in the region very close to the leading edge, but is not relevant to the streamline-curvature instability discussed above, because the main properties of their disturbance are similar to those of Poll's (1979) solutions of the Orr–Sommerfeld equation. To remove such restrictions, the present study has adopted an approximate equation system applicable to more general modes of disturbances, at the expense of mathematical rigorousness in the derivation of the disturbance equations. This has led us to success in revealing the possibility of two kinds of instabilities in the flow near the leading edge and in showing the principal effects of the angle of wing sweep and the curvature of the external streamlines. Such an approximate approach is meaningful for our understanding of fundamental aspects of physical phenomena and for providing approximate information useful for more rigorous analyses of the phenomena, for instance, by numerical simulations of the Navier–Stokes equations. It may be expected that the above results will be confirmed by numerical computations in the near future.

Since the streamline-curvature instability of general boundary-layer flows has not yet been detected in experiments, we have to look forward to future observations for more details of this new instability. The most important point to be pursued in experiments is probably the role of the streamline-curvature instability in the transitional process of three-dimensional boundary layers. It has been commonly believed that the transition from laminar to turbulence in three-dimensional flows is initiated by the cross-flow instability of the inflexion-point type, but the mechanism of initial development, namely the receptivity, of this kind of disturbances has not yet been clarified sufficiently. The streamline-curvature disturbances of the centrifugal type can grow at a much lower Reynolds number and bear a strong resemblance to the cross-flow disturbances, because their wavenumber vectors are both nearly perpendicular to external streamlines, like longitudinal vortices. It is, therefore, very likely that an interaction between the two kinds of disturbances is concerned in initial stage of transition. In association with this problem, it is also noteworthy that the centrifugal instability is very sensitive to external disturbances, as pointed out by Faller (*1991*) in a discussion of experimental results on rotating flows. Further investigations of the streamline-curvature instability seem to be necessary for a marked advance in the explanation of the receptivity process in three-dimensional boundary layers.

The author wishes to express his thanks to Dr S. Takagi for continuous and helpful discussion on the subject during the course of this study.

REFERENCES

BALAKUMAR, P. & MALIK, M. R. 1990 Traveling disturbances in rotating-disk flow. *Theoret. Comput. Fluid Dyn.* **2**, 125–137.

BALAKUMAR, P., MALIK, M. R. & HALL, P. 1991 On the receptivity and nonparallel stability of traveling disturbances in rotating-disk flow. *Theoret. Comput. Fluid Dyn.* **3**, 125–140.

FALLER, A. J. 1991 Instability and transition of disturbed flow over a rotating disk. *J. Fluid Mech.* **230**, 245–269.

FALLER, A. J. & KAYLOR, R. E. 1966 Investigations of stability and transition in rotating boundary layers. In *Dynamics of Fluids and Plasmas* (ed. S. I. Pai), pp. 309–329. Academic.

GREGORY, N., STUART, J. T. & WALKER, W. S. 1955 On the stability of three-dimensional boundary layers with application to the flow due to a rotating disk. *Phil. Trans. R. Soc. Lond.* A **248**, 155–199.

HALL, P. 1986 An asymptotic investigation of the stationary modes of instability of the boundary layer on a rotating disc. *Proc. R. Soc. Lond.* A **406**, 93–106.

HALL, P., MALIK, M. R. & POLL, D. I. A. 1984 On the stability of an infinite swept attachment line boundary layer. *Proc. R. Soc. Lond.* A **395**, 229–245.

ITOH, N. 1974 A power series method for the numerical treatment of the Orr–Sommerfeld equation. *Trans. Japan Soc. Aero. Space Sci.* **17**, 65–75.

ITOH, N. 1985 Stability calculations of the three-dimensional boundary layer flow on a rotating disk. In *Laminar-Turbulent Transition* (ed. V. V. Kozlov), pp. 463–470. Springer.

ITOH, N. 1991 Effect of pressure gradients on the stability of three-dimensional boundary layers. *Fluid Dyn. Res.* **7**, 37–50.

ITOH, N. 1994*a* Centrifugal instability of three-dimensional boundary layers along concave walls. *Trans. Japan Soc. Aero. Space Sci.* **37**, 125–138.

ITOH, N. 1994*b* Instability of three-dimensional boundary layers due to streamline curvature. *Fluid Dyn. Res.* **14**, 353–366.

ITOH, N. 1995 Effects of wall and streamline curvatures on instability of 3-D boundary layers. In *Laminar-Turbulent Transition* (ed. R. Kobayashi), pp. 323–330. Springer.

ITOH, N. 1996 Streamline-curvature instability of three-dimensional boundary layers. *Trans. Japan Soc. Aero. Space Sci.* in press.

LILLY, D. K. 1966 On the instability of Ekman boundary flow. *J. Atmos. Sci.* **23**, 481–494.

MACK, L. M. 1984 Boundary-layer linear stability theory. *AGARD Rep.* 709, pp. 3.1–3.81.

MALIK, M. R. 1986 The neutral curve for stationary disturbances in rotating-disk flow. *J. Fluid Mech.* **164**, 275–287.

POLL, D. I. A. 1979 Transition in the infinite swept attachment line boundary layer. *Aero. Q.* **30**, 607–629.

POLL, D. I. A. 1984 Transition description and prediction in three-dimensional flows. *AGARD Rep.* 709, pp. 5.1–5.23.

POLL, D. I. A. 1985 Some observations of the transition process on the windward face of a long yawed cylinder. *J. Fluid Mech.* **150**, 329–356.

REED, H. L. & SARIC, W. S. 1989 Stability of three-dimensional boundary layers. *Ann. Rev. Fluid Mech.* **21**, 235–284.

WATANUKI, T. & ITOH, N. 1984 Stability calculations of the two-dimensional boundary layer along a concave wall. *National Aerospace Lab. Rep.* NAL TR-841 (in Japanese).

WILSON, S. D. R. & GLADWELL, I. 1978 The stability of a two-dimensional stagnation flow to three-dimensional disturbances. *J. Fluid Mech.* **84**, 517–527.